This article has been accepted for publication in a future issue of this journal, but has not been fully edited. Content may change prior to final publication. Citation information: DOI 10.1109/JERM.2018.2817364, IEEE Journal of Electromagnetics, RF and Microwaves in Medicine and Biology

COMPACT MULTI-BAND WIRELESS ENERGY HARVESTING BASED BATTERY-FREE BODY AREA NETWORKS SENSOR FOR MOBILE HEALTHCARE

Liu Yang, Yong Jin Zhou, Chao Zhang, Xin Mi Yang, Xue-Xia Yang, and Chong Tan

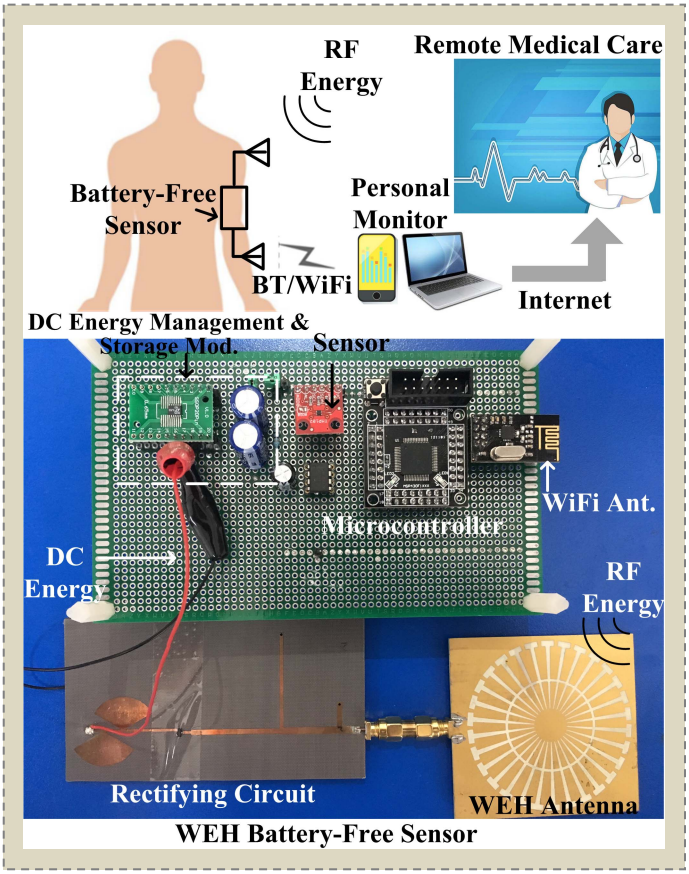

Future Application of Wireless Energy Harvesting based Battery-free Body Area Networks Sensor for Mobile Healthcare and a Prototype of a WEH Battery-free Sensor Node.

Take-Home Messages

- Ambient radio frequency (RF) energies in the air can be efficiently harvested to power a battery-free sensor node which may continuously communicate with personal monitor/remote medical staff through Bluetooth/WiFi or Internet for human body self-monitoring and mobile healthcare.
- We have demonstrated a prototype of a wirelessly powered battery-free body area networks (BAN) sensor for mobile healthcare, which consists of the electrically small triple-band rectenna, the direct current (DC) energy management and storage module, the microcontroller, and the sensing and communication module.
- The electrically small triple-band rectenna covers GSM-900, UTMS-2100, and TD-LTE bands, which has successfully supplied power for the battery-free body area networks sensor node.
- The electrical size of the antenna is only $0.21\lambda \times 0.2\lambda$, while the gains reach 1 dBi, 2.64 dBi, and −0.19 dBi at the operating frequencies 0.9 GHz, 2.025 GHz, and 2.36 GHz, respectively. The measured conversion efficiency remains 47% when the input power is −11.1 dBm.

This article has been accepted for publication in a future issue of this journal, but has not been fully edited. Content may change prior to final publication. Citation information: DOI 10.1109/JERM.2018.2817364, IEEE Journal of Electromagnetics, RF and Microwaves in Medicine and Biology

COMPACT MULTI-BAND WIRELESS ENERGY HARVESTING BASED BATTERY-FREE BODY AREA NETWORKS SENSOR FOR MOBILE HEALTHCARE

Liu Yang, Yong Jin Zhou, Chao Zhang, Xin Mi Yang, Xue-Xia Yang, and Chong Tan

Abstract: This paper demonstrates a prototype of a self-sustained body area networks (BAN) sensor, which consists of the electrically small triple-band rectenna, the direct current (DC) energy management and storage module, the microcontroller, and the sensing and communication module. The proposed antenna is composed of corrugated metal-insulator-metal (MIM) plasmonic structures, which covers triple frequency bands, including GSM-900, UTMS-2100, and TD-LTE bands. Its electrical size is only $0.21\lambda \times 0.2\lambda$ at 900 MHz. The gains reach 1 dBi, 2.64 dBi, and −0.19 dBi at 0.9 GHz, 2.025 GHz, and 2.36 GHz, respectively. A triple-band rectifier for low power application is designed to convert the harvested radio frequency (RF) power into DC power. The maximum RF to DC conversion efficiency of the rectifier reaches 59% when the input power is −10 dBm. The proposed compact BAN sensor based on multiband wireless energy harvesting is suitable for human body self-monitoring and mobile healthcare.

Keywords **—Energy harvesting, Body sensor networks, Rectenna, Rectifiers, Plasmons**

I. INTRODUCTION[1]

Mobile healthcare is getting more and more attention for prevention and better management of chronic diseases, nursing care of the aging society, and saving medical expenses [1]. The key technologies for mobile healthcare or remote medical care are body area networks (BAN) for the real-time monitoring of various physiological signals of human body [2]. Nevertheless, the BAN must have smaller nodes relative to a conventional wireless sensor networks (WSN) for comfortable user experience [3]. Smaller nodes imply smaller batteries, creating strict tradeoffs between the consumed energy and the performance. The capacity of the high energy density of lithium-based batteries is limited in diminutive BAN enclosures. The need to replace or recharge batteries frequently makes BAN less desirable, which will hamper the widespread adoption of these devices in daily healthcare [4]. The self-sustainable BAN has the potential to pave the road towards the massive utilization of wireless wearable sensors [5]-[6]. In this context, energy harvesting (EH) technologies, which take energy from ambient sources (such as mechanical, thermal, and electromagnetic (EM) sources), are used to power autonomous wireless systems [6]. Wireless energy harvesting (WEH) is to harvest surrounding EM energy to supply continuous power to the self-sustainable standalone devices [7], which provides a solution to replace the battery or save maintenance cost. Although the main drawback of WEH is the low power density [8], the available ambient wireless sources keep increasing due to the ever expanding wireless communication and broadcasting infrastructure. Moreover, ambient EM energies are available at all day and night. Hence, EM energy becomes a relatively reliable and steady ambient energy source, which has been applied to wireless structural health monitoring sensors [9], continuous health monitoring sensors [10], biotelemetry communication [11], etc. Dedicated radio frequency (RF) sources are necessary for the wirelessly powered wearable sensors in [10]-[14]. Here we focus on harvesting ambient RF energy from the air to power a BAN battery-free sensor node which may continuously communicate with personal monitor/remote medical staff through BT/WiFi or Internet (see Fig. 1(a)).

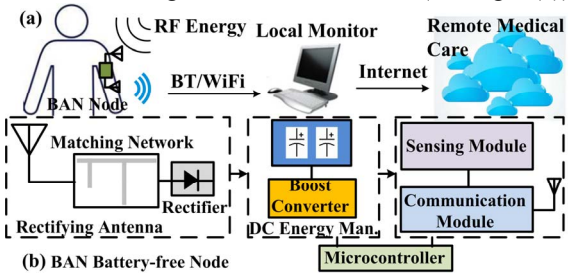

Fig. 1. (a) Future application of WEH battery-free sensor networks for daily healthcare. (b) Block diagram of a BAN battery-free node.

This paragraph of the first footnote will contain the date on which you submitted your paper for review. This work was supported in part by the National High-Tech Research Development Plan (863 plan) under Grant No. 2015AA016201, in part by Science and Technology Commission Shanghai Municipality (STCSM) under Grants No. SKLSFO2017-05 and No. 13ZR1454500. Corresponding Author is Y. J. Zhou.

L. Yang, C. Zhang, and X. –X. Yang are with the School of Communication and Information Engineering, Shanghai University, Shanghai 200444, China.

Y. J. Zhou is with the Key Laboratory of Specialty Fiber Optics and Optical Access Networks, Joint International Research Laboratory of Specialty Fiber Optics and Advanced Communication, Shanghai Institute for Advanced Communication and Data Science, Shanghai University, Shanghai 20044, China and also with State Key Laboratories of Transducer Technology, Chinese Academy of Sciences, Shanghai 200050, China (e-mail: yjzhou@shu.edu.cn).

X. M. Yang is with Soochow University, Suzhou 215006, China.

C. Tan is with the Shanghai Institute of Microsystem and Information Technology, Chinese Academy of Sciences, Shanghai 200050, China.

This article has been accepted for publication in a future issue of this journal, but has not been fully edited. Content may change prior to final publication. Citation information: DOI 10.1109/JERM.2018.2817364, IEEE Journal of Electromagnetics, RF and Microwaves in Medicine and Biology

Figure 1(b) shows the block diagram of a typical BAN battery-free sensor node, which is composed of a rectifying antenna, a DC energy management and storage module, a microcontroller, a sensing module, and a communication module. The rectifying-antenna (rectenna) that converts the incident EM power into direct current (DC) power is the most vital device for the WEH system. Ambient EM signals are normally distributed over various frequency bands [15]. A multiband or broadband rectenna is desirable to effectively capture the free energy from these frequency bands simultaneously. To design a multiband or broadband rectenna is very challenging, since the input impedance of the rectifier circuit varies as a function of the operating frequency, input power level, and load impedance. High efficiency multiband and broadband rectennas have been proposed [16]-[18], however, there are still various limitations. Firstly, due to BAN node placement variability and uncertainty about the user's exposure to ambient energy, the antenna for WEH should be of wide half power beamwidth to harvest ambient energy incident from random angles. Secondly, the BAN nodes are generally smaller (less area covered) and have fewer opportunities for redundancy [3]. Hence, compared to the rectifier circuit, power management system, or sensor module, the volume of the antenna for WEH is too large [19]-[20] and it should be electrically small. A wideband rectenna operating within 900-2450 MHz for wearable sensors in outdoor environments was introduced in [21]. However, the rectenna is not compact and its size is large. A fully-autonomous integrated RF energy harvesting system for wearable applications was described, which harvests RF energy from GSM 900/1800 and wireless fidelity in 2.4 GHz on user request [22]. However, the harvesting antenna is still a little large (150 mm × 150 mm).

In this paper, a novel electrically small triple band rectenna has been proposed, which works at GSM-900, UTMS-2100, and TD-LTE bands. The antenna is composed of corrugated metal-insulator-metal (MIM) plasmonic structures and its electrical size is only $0.21\lambda \times 0.2\lambda$ (66mm × 70 mm) at 900MHz. A triple-band low-power rectifier has also been proposed and combined with the antenna. The simulated peak efficiencies are 59%, 49%, 48% at the frequencies of 0.9 GHz, 2.025 GHz, 2.36 GHz, respectively, when the input power is −10 dBm. The measured RF to DC conversion efficiencies at 2.025 GHz agree well with the simulation results. When the input power is decreased to −11.1 dBm, the efficiency remains 47%. A prototype of a self-sustained body area sensor networks node has been demonstrated, where the electrically small triple-band rectenna has successfully supplied power for the node consisting of the DC energy management and storage module, the microcontroller, and the sensing and communication module. The proposed compact multiband WEH system is suitable for human body self-monitoring and daily healthcare.

II. Antenna Design

Metamaterials are composed of sub-wavelength particles that can achieve parameters not possible within naturally occurring materials. Recently, metamaterials are also used to harvest EM energy in the microwaves regime, including a flower-like structure composed of four electrically small split-ring resonators (SRRs) [23], a circular slotted truncated corner square patch radiator placed on reactive impedance surface (RIS) [24], a parallel connection of five SRRs loaded with embedded devices [25], etc. However, the previous design was mainly for a single narrow frequency band and required a relatively high input power level. Loop antennas over artificial magnetic conductor surface for dual-band energy harvesting have been proposed [26]. But the size of the antenna is not compact. Since spoof surface plasmons (SPs) are not constrained by the diffraction limit and can achieve subwavelength confinements to the EM waves [27], they have important potential applications in the miniaturization of spoof plasmonic circuits. Many antennas based on spoof SPPs have been demonstrated [28]-[29]. While the near field characteristics of spoof LSPs have been fully investigated [30]-[31], their far field behaviors are still unknown. To our knowledge, only a sub-wavelength unidirectional antenna was designed by combining two spoof LSPs resonators [32].

Here we propose a multiband antenna based on spoof LSPs resonator, as shown in Fig. 2(a), which is composed of an annular ring slot and periodic array of T-shaped grooves. The corrugated slot line ring is printed on the substrate (Rogers RO4350), with relative dielectric constant of 3.48 and loss tangent of 0.004. It is fed by a 50-Ω microstrip line. The metal disk at the end of the microstrip conductor is used to increase the coupling degree of electromagnetic energy. The fabricated multiband antenna based on spoof LSPs resonator is shown in Fig. 2(b).

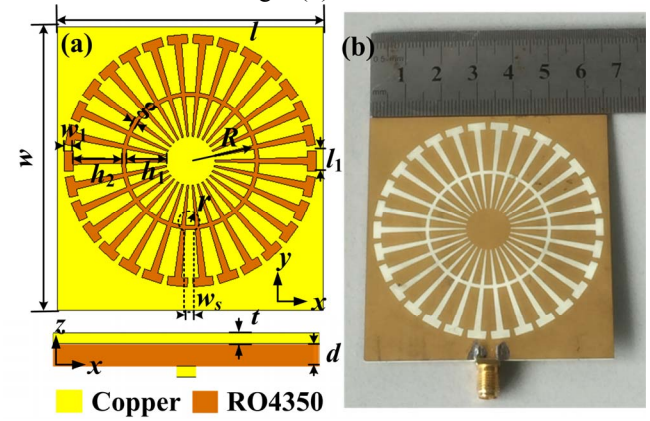

Fig. 2. (a) Front view and side view of the antenna. Dimensions: l = 66 mm, w = 70 mm, R = 16 mm, h_1 = 10 mm, h_2 = 12 mm, w_1 = 2.2 mm, l_1 = 5 mm, g = 1 mm, r = 2.85 mm, w_s = 2.33 mm, t = 0.018 mm, d = 1.016 mm. (b) Photograph of the fabricated antenna.

In order to illustrate the influences of the grooves with different shapes, three different structures are shown in Fig. 3. Structure I is the conventional slot line ring. Structure II and III are the corrugated slot line ring with periodic array of

This article has been accepted for publication in a future issue of this journal, but has not been fully edited. Content may change prior to final publication. Citation information: DOI 10.1109/JERM.2018.2817364, IEEE Journal of Electromagnetics, RF and Microwaves in Medicine and Biology

rectangle grooves and T-shaped grooves, respectively. The dispersion curves for these three kinds of waveguides are calculated by use of the eigenmode solver of the commercial software, CST Microwave Studio. They are plotted in Fig. 4(a). It can be seen that the dispersion curve is lowered when the slot is corrugated. That means that the operating frequency of structure III will be the lowest when the wave vector β is fixed, since its dispersion curve is the lowest.

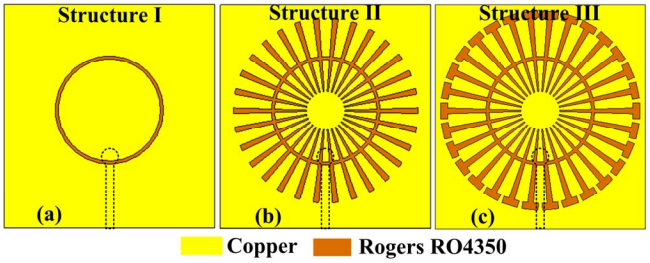

Fig. 3. Different structures based on the slot ring.

It is known that the slot ring resonator antenna can form multimode resonances. For the above three different structures based on the slot ring, the circumference L of the slot ring and the multimode guided wavelength λ_n satisfy $L \approx n \times \lambda_n (n = 1, 2, 3...)$, where n is a positive integer (corresponding to the resonant modes). For a fixed L (R = 16 mm), the guided wavelength λ_n at the multiple resonance modes can be calculated from the above equation. Then we can get β_n by $\beta_n = 2\pi/\lambda_n$ and the operating resonant frequency can be obtained from the dispersion curves in Fig. 4(a). The simulated reflection coefficients using CST time domain solver are presented in Fig. 4(b). We can see that the resonant frequency of the first mode for the structure III is indeed the lowest, much lower than that of the first mode for the structure I. This indicates that more compact resonator antennas can be achieved based on such spoof plasmonic structures.

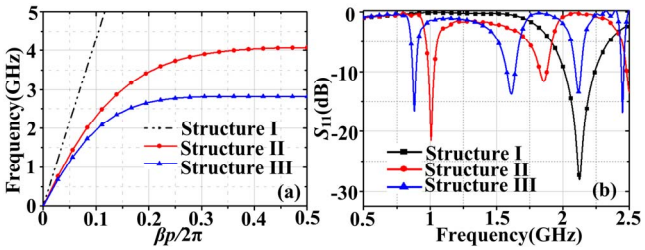

Fig. 4. (a) Dispersion curves of the three structures and (b) simulated reflection coefficients of the three structures I-III.

The reflection coefficients for different h_2 are plotted in Fig. 5(a). It can be seen that the resonant frequencies red shift when h_2 is gradually increased from 10 mm to 12 mm. However, the offset is different for different resonant modes, which indicates that we can control the resonant frequencies by tuning the geometrical parameters. The reflection coefficients of the multiband antenna are measured by a vector network analyzer (Agilent N5227A), which are shown in Fig. 5(b). It can be observed that the measured result agrees well with the simulated one. The result shows that there are four resonant modes marked as m_1-m_4. The corresponding resonant frequencies are 0.9 GHz, 1.575 GHz, 2.025 GHz and 2.36 GHz, which include the GSM-900, UTMS-2100 and TD-LTE bands. Hence, the electrical size of the antenna is only $0.21\lambda \times 0.2\lambda$ at 0.9 GHz.

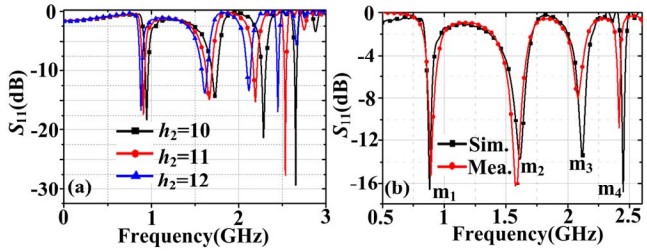

Fig. 5. (a) Simulated reflection coefficients for different h_2. (b) Simulated and measured reflection coefficients.

The radiation patterns of E-plane at the four resonant frequencies are simulated and measured, as shown in Fig. 6. The proposed multiband antenna exhibits radiation characteristics similar to the dipole antenna in all frequency bands, with broad half power beamwidth, since the electrical size are 0.2λ, 0.35λ, 0.45λ, and 0.52λ at 900 MHz, 1.575 GHz, 2.025 GHz and 2.36 GHz, respectively. The measured antenna gains are 1 dBi, 1.6 dBi, 2.64 dBi and −0.19 dBi at 0.9 GHz, 1.575 GHz, 2.025 GHz and 2.36 GHz, respectively. The measured radiation efficiencies are 42.2%, 61.3%, 72.6%, 32.8% at 0.9 GHz, 1.575 GHz, 2.025 GHz and 2.36 GHz, respectively. The gain is expected to increase when the operating frequency is increased, due to the increased electrical size.

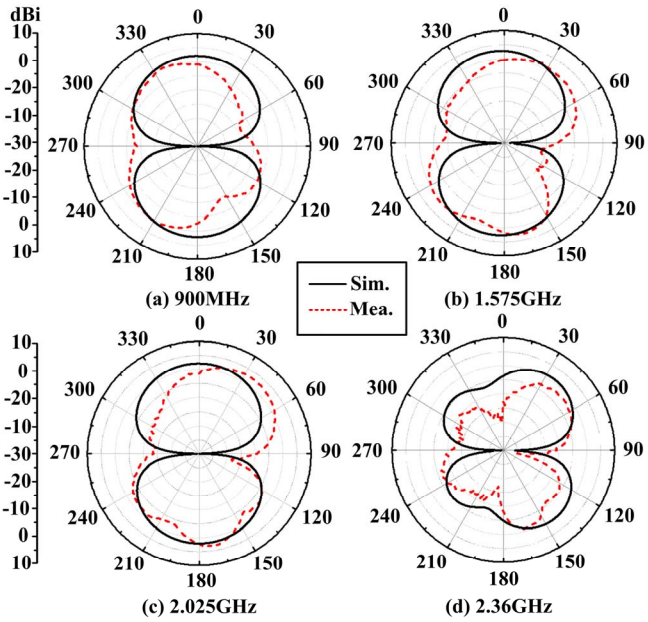

Fig. 6. Simulated and measured radiation patterns at (a) 0.9 GHz, (b) 1.575 GHz, (c) 2.025 GHz, and (d) 2.36 GHz.

In order to explain why the gain and radiation efficiency at 2.36 GHz are lower, we have conducted more simulations and found that the high-order mode (2.36 GHz) is more sensitive to the metal loss and dielectric loss than the other modes. First, when the metal is changed from perfect conductor (PEC) to copper, the radiation efficiencies at m_2

This article has been accepted for publication in a future issue of this journal, but has not been fully edited. Content may change prior to final publication. Citation information: DOI 10.1109/JERM.2018.2817364, IEEE Journal of Electromagnetics, RF and Microwaves in Medicine and Biology

and m_3 decrease 1.1% and 4.9%, respectively, while the efficiency at m_4 decreases 7.6%. When the loss tangent of the dielectric substrate is changed from 0.004 to 0.01 (the metal is still copper), the efficiencies at m_2 and m_3 decrease 3.2% and 9.7%, respectively, while the efficiency at m_4 decreases 15.8%. Hence, the m_4 mode (2.36 GHz) is more sensitive to the metal loss and dielectric loss, which may lead to the decreased radiation efficiency and gain.

The comparison between this work and some typical designs is given in Table I. The goal is to harvest energy from GSM-900, UTMS-2100 and TD-LTE bands simultaneously. Hence 1.575 GHz is not listed. We can see that for the multiband antenna, our design is very compact and the electrical size is only $0.21\lambda \times 0.2\lambda$ at 0.9 GHz.

TABLE I
COMPARISION BETWEEN OUR DESIGN AND OTHERS'

Ref.	Frequency (GHz)	Size (mm^2)	Gain (dBi)
15	1.8-2.5	70×70	2.5, 3.5, 3.8
17	0.9, 1.75, 2.15, 2.45	155×155	9.8, 5, 4.8, 9.6
18	0.55-2.5	160×160	2.5~5
26	0.5, 0.875	500×500	8.2, 8.5
This work	0.9, 2.025, 2.36	66×70	1, 2.64, −0.19

III. Rectifier Design And Measurement

Although rectifiers based on CMOS technology are compact and can work at very low input power, they operate only at single band [33]-[34]. The rectifier using PCB technology is easy to be integrated with printed circuits and antennas can be designed to operate at multiple frequency bands [35]. Here a simple triple-band rectifier based on PCB technology is demonstrated. The substrate is F4B-2 with relative dielectric constant of 2.65 and loss tangle of 0.001, whose thickness is 0.8 mm. The layout of the tripe-band rectifier is shown in Fig. 7 and the inset gives the photograph of the fabricated rectifier. The rectifier is composed of an impedance match network (IMN), a Schottky diode, a DC-pass filter and a resistive load. The diode HSMS-2850 is suitable for the low power application, whose threshold and breakdown voltages are 0.15 V and 3.8 V. However, its impedance is complex and frequency dependent. A closed-form solution to match a frequency dependent complex impedance load to a real impedance source at two arbitrary frequencies by using T-shaped transmission lines has been introduced in [36]. With the T-shaped structure (TL_0, TL_1 and TL_6 in Fig. 7), the impedance match at the first resonant frequency (around 0.9 GHz) and the last resonant frequency (around 2.36 GHz) is achieved. However, this approach can match at only two frequency points. Therefore, to match the diode in triple-band, another T-shaped structure (TL_1, TL_2 and TL_7 in Fig. 7) is adopted, which mainly affects the impedance match at the other resonant frequency (around 2.025GHz). Hence, the final IMN consists of two T-shape transmission lines and the final optimized parameters of the rectifier by use of HFSS are provided in the caption of Fig. 7. The DC-pass filter is composed of two cascaded radial open stubs, which is used to block the fundamental wave and the harmonics and to smooth the output DC power. The resistive load of 2 kΩ is attached to the output port for collecting the DC power.

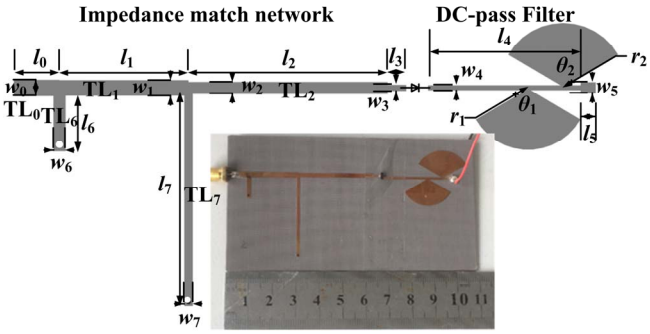

Fig. 7. The layout and photograph of the rectifier. The parameters: w_0 = 2.64 mm, w_1 = 2.52 mm, w_2 = 1.92 mm, w_3 = 1 mm, w_4 = 1 mm, w_5 = 2.2 mm, w_6 = 2 mm, w_7 = 1.4 mm, l_0 = 7.5 mm, l_1 = 21.2 mm, l_2 = 32.7 mm, l_3 = 3.05 mm, l_4 = 30.5 mm, l_5 = 3 mm, l_6 = 8 mm, l_7 = 33.8 mm, $\theta_1 = \theta_2$ = 120, r_1 = 11.5 mm, r_2 = 12.1 mm.

The simulations were carried out by use of the software Advanced Design System (ADS). The simulated and measured reflection coefficients of the rectifier are shown in Fig. 8 (a). Compared with the simulated result, the measured one has a slight shift, which may be caused by the manual welding process. Figure 8(b) shows the simulated conversion efficiency versus frequency at the input power of −10 dBm. The simulated peak efficiencies are 59%, 49%, 48% at the frequencies of 0.9 GHz, 2.025 GHz, 2.36 GHz, respectively. It can be seen that the conversion efficiency of the rectifier is good. However, the dimension of the rectifier is still big, compared to the electrically small antenna. In the next work, the dimension of the rectifier can be miniaturized by use of metamaterials [37], lumped elements [38], stacked multilayer structure [39], and so on.

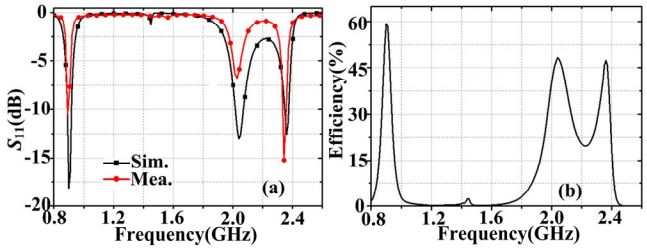

Fig. 8. (a) Simulated and measured S_{11} of the rectifier. (b) The simulated conversion efficiency versus frequency at the input power of −10 dBm.

IV. Rectenna Measurement

By combing the antenna with the rectifier, a multiband rectenna can be achieved. The experiment was carried out in an anechoic chamber. The measurement system is illustrated in Fig. 9 (a). The distance between the standard horn antenna and the proposed antenna meets the far field requirement. The received power P_r of the proposed antenna is marked in Fig. 9(a) and was measured by a power meter. Then, the antenna was replaced by the rectenna at the same position. Hence, the input power to the rectifier can be substituted by the received power P_r. By this means, the use of Friis

This article has been accepted for publication in a future issue of this journal, but has not been fully edited. Content may change prior to final publication. Citation information: DOI 10.1109/JERM.2018.2817364, IEEE Journal of Electromagnetics, RF and Microwaves in Medicine and Biology

transmission equation can be avoided. By measuring the voltages across the resistor, the conversion efficiency η can be obtained by

$$\eta = \frac{V_L^2}{R_L} \times \frac{1}{P_r} \times 100\% \quad (1)$$

where V_L is the voltage on the resistor, R_L is the resistance value (2 kΩ).

The simulated and measured RF to DC conversion efficiency versus the input power to the rectifier at 2.025 GHz is depicted in Fig. 9 (b). It can be seen that when the input power to the rectifier is 0 dBm, the simulated RF to DC conversion efficiency achieves its peak value of 58%. When the input power is −11.1 dBm, the measured efficiency is 47%. Due to the maximum input power limit of the amplifier in our laboratory, the obtained measured input power is below −5 dBm. It can be seen that the measured results agree well with the simulated results.

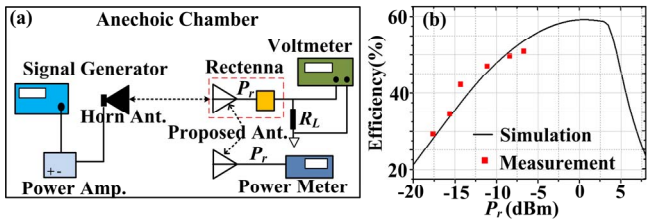

Fig. 9. (a) The measurement system. (b) The simulated and measured conversion efficiency versus input power at 2.025 GHz.

V. BAN Node Design

After designing and developing the WEH harvester, an additional goal is to use this energy to supply a BAN node. The node consists of four main blocks: the rectenna, the DC energy management and storage module, the microcontroller, and the sensing and communication module, as shown in Fig.9. Since the output voltage from the RF energy harvester depends on the quantity of cellular communications traffic and is only 0.65 V when the input RF power is −10 dBm and the load is 2 MΩ, a DC/DC boost converter is necessary to control the voltage that is delivered to the capacitor from the rectifier circuit. The boost converter is based on a high efficiency step-up DC/DC chip (LTC3105, Linear Tech.), which can operate from input voltages as low as 225 mV. The maximum power point control (MPPC) circuit integrated in LTC3105 allows the user to set the optimal input voltage operating point for a given power source, which dynamically regulates the average inductor current to prevent the input voltage from dropping below the MPPC threshold. The MPPC pin voltage is set by connecting a resistor between the MPPC pin and GND, which is determined by the equation: $V_{MPPC} = 10\mu A \bullet R_{MPPC}$. For example, when the input start-up voltage is 0.65 V, it is easy to calculate the necessary resistance to program the activation point for the MPPC loop. Peak current limits are automatically adjusted with proprietary techniques to maintain operation at levels that maximize power extraction from the source according to the LTC3105 datasheet. The DC/DC converter is then connected to the energy storage module. Conventional rechargeable battery-based energy storage systems present some disadvantages by not allowing a precise estimation of the remaining energy, having a limited number of recharge/discharge cycles, and higher environmental impact when batteries are improperly disposed [27]. Here a super-capacitor storing system for the energy harvested from the EM waves is developed. After it achieves a stable voltage in the super-capacitor bank, the microcontroller (MSP430F149, TI) starts using the energy stored in the super-capacitor bank in order to self-sustain its management activity. The microcontroller can work at a minimum voltage of 1.8 V. Its operating current is 0.7 μA in standby mode and the current is 0.28 mA for active mode. The temperature data collected by the digital temperature chip (TMP102, TI) is delivered to the communication module (nRF24L01, Nordic) under the control of the microcontroller. The maximum standby current of TMP102 is only 10μA. The operating current of nRF24L01 does not exceed 10 mA.

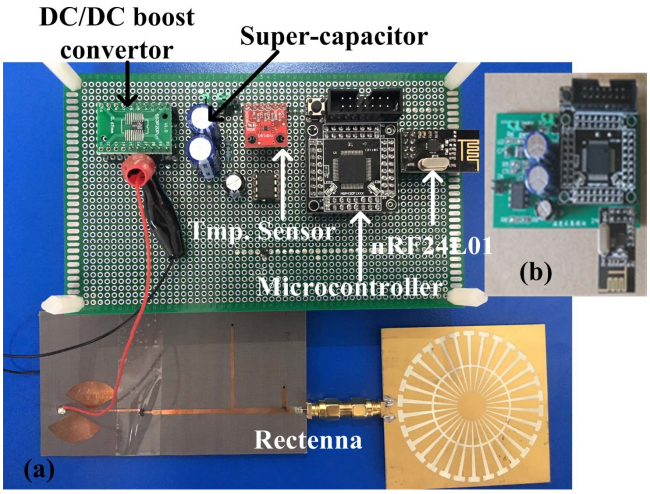

Fig. 10. (a) The photograph of the BAN node. (b) The fabricated integrated sensor node.

VI. Conclusion

An electronically small multiband rectenna covering GSM-900, UTMS-2100 and TD-LTE triple bands has been demonstrated. For the multiband antenna, our design is very compact and the electrical size is the smallest in comparisons with other existing designs. Its electrical size is only $0.21\lambda \times 0.2\lambda$ at 0.9 GHz, while the gains remain 1 dBi, 2.64 dBi, and −0.19 dBi at the operating frequencies 0.9 GHz, 2.025 GHz, and 2.36 GHz, respectively. A triple-band rectifier is optimized to match the antenna. The measured RF to DC conversion efficiency remains 47% when the input power is −11.1 dBm. A prototype of a battery-free BAN node has been demonstrated, where the rectenna has successfully supplied power for the node consisting of the DC energy management and storage module, the microcontroller, and the sensing and communication module. The proposed compact sensor based on multiband WEH is suitable for human body self-monitoring and mobile healthcare. More compact

sensor with miniaturized rectifying circuit and stacked multilayer structure is still under development.

REFERENCES

[1] A. Darwish and A. Hassanien, "Wearable and implantable wireless sensor network solutions for healthcare monitoring," *Sensors*, vol. 11, no. 6, pp. 5561–5595, June 2011.

[2] B. Latre, B. Braem, I. Moerman, C. Blondia, and P. Demeester, "A survey on wireless body area networks," *Wireless Netw.*, vol. 17, no. 1, pp. 118, January 2011.

[3] M. A. Hanson, H.C. Jr. Powell, A.T. Barth, K. Ringgenberg, B. H. Calhoun, J. H. Aylor, and J. Lach, "Body area sensor networks: challenges and opportunities," *Computer*, vol. 42, pp. 58-65, Jan. 2009.

[4] L. M. Borges, R. Chávez-Santiago, N. Barroca, F. J. Velez, and I. Balasingham, "Radio-frequency energy harvesting for wearable sensors," *Healthcare Technol. Lett.*, Vol. 2, pp. 22-27, Feb. 2015.

[5] B. Lo, S. Thiemjarus, A. Panousopoulou, and G. Z. Yang, "Bioinspired design for body sensor networks [life sciences]," *IEEE Signal Process. Mag.*, vol. 30, pp. 165-170, Dec. 2013.

[6] D. Gündüz, K. Stamatiou, N. Michelusi, and M. Zorzi, "Designing intelligent energy harvesting communication systems," *IEEE Commun. Mag.*, vol. 52, pp. 210-216, Jan. 2014.

[7] S. Kim, R. Vyas, J. Bito, K. Niotaki, A. Collado, A. Georgiadis, and M. M. Tentzeris, "Ambient RF energy-harvesting technologies for self-sustainable standalone wireless sensor platforms," *Proc. IEEE*, vol. 102, pp. 1649-1666, Oct. 2014.

[8] A. Harb, "Energy harvesting: State-of-the-art," *Renewable Energy*, vol. 36, pp. 2641-2654, Oct. 2011.

[9] X. Y. Wang and A. Mortazawi, "Medium wave energy scavenging for wireless structural health monitoring sensors," *IEEE Trans. Micro. Theory Techn.*, vol. 62, pp. 1067-1073, Feb. 2014.

[10] J. Yoo, L. Yan, S. Lee, Y. Kim, and H. J. Yoo, "A 5.2 mW self-configured wearable body sensor network controller and a 12μw wirelessly powered sensor for a continuous health monitoring system," *IEEE J. Solid-State Circuits*, vol. 45, pp. 178-188, Dec. 2010.

[11] F. Huang, C. Lee, C. Chang, L. Chen, T. Yo, and C. Luo, "Rectenna application of miniaturized implantable antenna design for triple-band biotelemetry communication," *IEEE Trans. Antennas Propag.*, vol. 59, pp. 2646-2653, May 2011.

[12] S. Mandal, L. Turicchia, and R. Sarpeshkar, "A low-power, battery-free tag for body sensor networks," *IEEE Pervasive Comput.*, vol. 9, pp. 1536-1268, Dec. 2009.

[13] X. Zhang, H. Jiang, L. Zhang, C. Zhang, Z. Wang, and X. Chen, "An energy-efficient ASIC for wireless body sensor networks in medical applications," *IEEE Trans. Biomed. Circuits Syst.*, vol. 4, pp. 11-18, Nov. 2010.

[14] L. Xia, J. Cheng, N. E. Glover, and P. Chiang, "0.56 V, -20 dBm RF-powered, multi-node wireless body area network system-on-a-chip," *IEEE J. Solid-State Circuits*, vol. 49, pp. 1345-1355, Feb. 2014.

[15] C. Song, Y. Huang, J. Zhou, J. Zhang, S. Yuan, and P. Carter, "A high efficiency broadband rectenna for ambient wireless energy harvesting," *IEEE Trans. Antennas Propag.*, vol. 63, pp. 3486-3495, May 2015.

[16] N. Shariati, W. S. T. Rowe, J. R. Scott, and K. Ghorbani, "Multi-service highly sensitive rectifier for enhanced RF energy scavenging," *Sci. Rep.*, vol. 5, May 2015.

[17] D. Masotti, A. Costanzo, M. Del Prete, and V. Rizzoli, "Genetic-based design of a tetra-band high-efficiency radio-frequency energy harvesting system," *IET Microw. Antennas Propag.,* vol. 7, pp. 1254-1263, Dec. 2013.

[18] C. Y. Song, Y. Huang, P. Carter, J. F. Zhou, S. Yuan, Q. Xu, and M. Kod, "A novel six-band dual CP rectenna using improved impedance matching technique for ambient RF energy harvesting," *IEEE Trans. Antennas Propag.*, vol. 64, pp. 3160-3171, May 2016.

[19] H. Sun, Y. X. Guo, M. He, and Z. Zhong, "A dual-band rectenna using broadband Yagi antenna array for ambient RF power harvesting," *IEEE Antennas Wireless Propag. Lett.*, vol. 12, pp. 918-921, Jul. 2013.

[20] V. Kuhn, C. Lahuec, F. Seguin, and C. Person, "A multi-band stacked RF energy harvester with RF-to-DC efficiency up to 84%," *IEEE Trans. Microw. Theory Techn.*, vol. 63, pp. 1768-1778, Apr. 2015.

[21] V. Kuhn, F. Seguin, C. Lahuec, and C. Person, "A multi-tone RF energy harvester in body sensor area network context," in *Antennas Propag. Conf. (LAPC)*, Loughborough, 2013, pp. 238-241.

[22] M. Dini, M. Filippi, A. Costanzo, A. Romani, M. Tartagni, M. D. Prete, and D. Masotti, " A fully-autonomous integrated RF energy harvesting system for wearable applications," in *Microwave Conf. (EuMC)*, European, 2013, pp. 987-990.

[23] M. R. AlShareef, and O. M. Ramahi, "Electrically small particles combining even-and odd-mode currents for microwave energy harvesting," *Appl. Phys. Lett.*, vol. 104, Jun. 2014.

[24] K. Agarwal, T. Mishra, M. F. Karim, Nasimuddin, M. O. L. Chuen, Y. X. Guo, and S. K. Panda, "Highly efficient wireless energy harvesting system using metamaterial based compact CP antenna," in *Microwave Symp. Digest (IMS)*, 2013 *IEEE MTT-S International*, pp. 1-4.

[25] A. M. Hawkes, A. R. Katko, and S. A. Cummer, "A microwave metamaterial with integrated power harvesting functionality," *Appl. Phys. Lett.*, vol. 103, pp. 163901, Sept. 2013.

[26] H. Kamoda, S. Kitazawa, Naoya Kukutsu and K. Kabayashi, "Loop antenna over artificial magnetic conductor surface and its application to dual-band RF energy harvesting," *IEEE Trans. Antennas Propag.*, vol. 63, pp. 4408-4417, Jul. 2015.

[27] E. Ozbay, "Plasmonics: merging photonics and electronics at nanoscale dimensions," *Science*, vol. 311, pp. 189-193, Jan. 2006.

[28] J. J. Wu, D. J. Hou, H. L. Chiueh, J. Q. Shen, C. J. Wu, Y. H. Kao, W. C. Lo, T. J. Yang, and C. J. Wu, "Kind of high directivity scanning radiation based on subwavelength periodic metal structure," *Electron. Lett.*, vol. 50, pp.1611-1613, Oct. 2014.

[29] A. Kianinejad, Z. N. Chen, and C. W. Qiu, "A single-layered spoof-plasmon-mode leaky wave antenna with consistent gain," *IEEE Trans. Antennas Propag.*, vol. 65, pp.681-687, 2017.

[30] A. Pors, E. Moreno, L. Martin-Moreno, J. B. Pendry, and F. J. Garcia-Vidal, "Localized spoof plasmons arise while texturing closed surfaces," *Phys. Rev. Lett*., vol. 108, 223905, May 2012.

[31] X. Shen, and T. J. Cui, "Ultrathin plasmonic metamaterial for spoof localized surface plasmons," *Laser Photonics Rev.*, vol. 8, no. 1, 137, Nov. 2014.

[32] F. Qin, Q. Zhang, and J. J Xiao, "Sub-wavelength Unidirectional Antenna Realized by Stacked Spoof Localized Surface Plasmon Resonators," *Sci. Rep.*, vol. 6, Jul. 2016.

[33] C.-J. Li and T.-C. Lee, "2.4-GHz high-efficiency adaptive power," *IEEE Trans. Very Large Scale Integr. (VLSI) Syst.*, vol. 22, no. 2, pp. 434-438, Feb. 2014.

[34] S. Scorcioni, L. Larcher, and A. Bertacchini, "A reconfigurable differential CMOS RF energy scavenger with 60% peak Efficiency and -21dBm sensitivity," *IEEE Microw. Wireless Compon. Lett.*, vol. 23, no. 3, pp. 155-157, Mar. 2013.

[35] J. J. Lu, X. X. Yang, H. Mei, and C. Tan, "A four-band rectifier with adaptive power for electromagnetic energy harvesting," *IEEE Microw. Wirel. Co.*, vol. 26, pp. 819-821, Oct. 2016.

[36] M. A. Nikravan, and Z. Atlasbaf, "T-section dual-band impedance transformer for frequency-dependent complex impedance loads," *Electron. Lett.*, vol. 47, no. 9, pp. 551-553, Apr. 2011.

[37] S. Choi, A. Salim, H. Jeong, and S. Lim, "High-efficiency and compact metamaterial-inspired 900 MHz rectifier," *J. Microw. Power Electromagn. Energy*, vol. 50, no.3, pp. 168-181, 2016.

[38] C. Song, Y. Huang, J. Zhou, J. Zhang, S. Yuan, and P. Carter, "A high-efficiency broadband rectenna for ambient wireless energy harvesting," *IEEE Trans. Antennas Propag.*, vol. 63, no. 8, pp. 3486-3495, Aug. 2015.

[39] K. Niotaki, S. Kim, S. Jeong, A. Collado, A. Georgiadis, and M. M. Tentzeris, "A compact dual-band rectenna using slot-loaded dual band folded dipole antenna," *IEEE Antennas Wirel. Propag. Lett.*, vol. 12, pp. 1634-1637, 2013.

Liu Yang was born in Jiangsu, China, in 1993. She received the B. S. degree in Electronic and information engineering from school of communication and information engineering, Shanghai University, in 2015. She is currently working towards her M. S. degree in electromagnetic field and microwave technology at Shanghai University, where she conducts research on plasmonic metamaterials, antennas and other functional devices. She has authored or coauthored over 4 papers on the international academic journals.

This article has been accepted for publication in a future issue of this journal, but has not been fully edited. Content may change prior to final publication. Citation information: DOI 10.1109/JERM.2018.2817364, IEEE Journal of Electromagnetics, RF and Microwaves in Medicine and Biology

Yong Jin Zhou (S'08-M'11) was born in Shandong, China, in 1982. He received the B.S. degree from Shandong University, Jinan, China, in 2006, and the Ph.D. degree in electromagnetic field and microwave technology from Southeast University, Nanjing, China, in 2011. In 2012, he joined the key laboratory of specialty fiber optics and optical access networks, school of communication and information engineering, Shanghai University, China. Since March 2015, he became associate professor with school of communication and information engineering, Shanghai University. His research interests include plasmonic metamaterials, THz functional devices, metamaterials rectenna. He has authored or coauthored over 30 papers on international academic journals. He is a frequent reviewer for several scientific journals. He is now IEEE Member, OSA member and Chinese Institute of Electronics senior member.

Chao Zhang was born in Hunan, China, in April 1991. He received the B. S. degree in communication and information engineering from Huaihua College in 2014. He is currently working toward the M. S. degree in electromagnetic field and microwave technologies at Shanghai University. His research interests focus on plasmonic metamaterials and devices at microwave and THz frequencies. He has authored or coauthored over 6 papers on international academic journals and international conferences.

Xin Mi Yang was born in Suzhou, Jiangsu Province, China, in 1982. He received the B.S. and Ph.D. degrees from Southeast University, Nanjing, China, in 2005 and 2010, respectively, both in the School of Information Science and Engineering. In November 2010, he joined the School of Electronics and Information Engineering, Soochow University, Suzhou, China, and has been an associate professor since July 2014. He co-edited the book Metamaterials - Beyond Crystals, Noncrystals, and Quasicrystals (CRC Press, June 2016) and is the author of two book chapters. He has published journal articles in IEEE Transactions, Optics Letters etc. His current research interests include metamaterials, metasurfaces, LTCC technology and their applications on antennas and microwave engineering.

Xue-Xia Yang (M'05-SM'17) received the B.S. and M.S. degrees from Lanzhou University, Lanzhou, China, in 1991 and 1994, respectively, and the Ph.D. degree in electromagnetic field and microwave technology from Shanghai University, Shanghai, China, in 2001. From 1994 to 1998, she was a teaching assistant and a lecturer in Lanzhou University, China. From 2001 to 2008, she was a lecture and an associate professor in Shanghai University, China. She is currently a professor and the Head of the Antennas and Microwave R&D Center at Shanghai University. She has authored or coauthored over 150 technical journal and conference papers. She is also a frequent reviewer for over 10 scientific journals. Her research interests include antennas theory and technology, computational electromagnetics and microwave power transmission. She is now a member of the Committee of Antenna Society of China Electronics Institute and Senior Member of China Electronics Institute. She is an associate editor for the Journal of Shanghai University (Science edition).

Chong Tan was born in Jiangxi, China, in 1984. She received her M.S. and Ph.D. degrees in 2009 and 2013 from the school of communications and information engineering, Shanghai University. She is currently an associate professor in the laboratory of broadband wireless technology at Shanghai institute of microsystem and information technology CAS. Her research interests are in the area of large-scale networked systems, peer-to-peer networks, wireless sensor networks.